

Approximation of probability density functions for SPDEs using truncated series expansions⁰

Giacomo Capodaglio*

Max Gunzburger*

Henry P. Wynn[†]

Abstract

The probability density function (PDF) of a random variable associated with the solution of a stochastic partial differential equation (SPDE) is approximated using a truncated series expansion. The SPDE is solved using two stochastic finite element (SFEM) methods, Monte Carlo sampling and the stochastic Galerkin method with global polynomials. The random variable is a functional of the solution of the SPDE, such as the average over the physical domain. The truncated series are obtained considering a finite number of terms in the Gram-Charlier or Edgeworth series expansions. These expansions approximate the PDF of a random variable in terms of another PDF, and involve coefficients that are functions of the known cumulants of the random variable. To the best of our knowledge, their use in the framework of SPDEs has not yet been explored.

1 Introduction

In the field of uncertainty quantification, the problem of describing the probability density function (PDF) of the output of a model, given a known distribution of the input is of major relevance [12]. For instance, for the solution of inverse problems involving partial differential equations (PDEs) with Bayesian inference [48, 18, 11], the PDF for the forward problem may be sought to get insights on the forward uncertainty propagation [34, 33]. The forward PDF is inferred from the histogram, which may be obtained according to two different strategies. The first is a direct approach, where Monte Carlo (MC) sampling is used to obtain realizations of the quantity of interest (QoI) by solving the forward problem for each sample. Alternatively, once an approximation of the stochastic solution of the forward problem is obtained, realizations may be obtained with MC sampling without solving the problem for each sample. This is the method used for instance in [34], where the stochastic solution of the forward problem is approximated with polynomial chaos, or in [33], where adaptive sparse grid collocation is employed. In this work, we propose an alternative strategy to estimate the PDF of a quantity of interest, given a known distribution for the input data. The quantities of interest are associated with the solution of a stochastic partial differential equation (SPDE), which is approximated using a stochastic finite element method (SFEM). Once the QoI has been obtained from the SPDE solution, its PDF is estimated by means of a truncated Gram-Charlier (GC) or Edgeworth (ED) series expansion [31]. These series have been used in several fields such as chemistry [41, 20], finance [29, 45, 37], physics and astrophysics [21, 19, 40, 30, 8, 15], material science [46], oceanology [53], power systems engineering [22], and other branches of applied mathematics [42]. However, to the best of our knowledge, their use in the field of SPDEs has not yet been explored. The GC and ED expansions approximate a PDF adding successive corrections to a known PDF that is used as a first approximation. The known PDF is usually chosen to be Gaussian, and only a few efforts have been made to generalize the GC expansion to the case of a non-Gaussian kernel [9, 7]. The terms in the GC and ED series involve derivatives of the known PDF and are functions of the cumulants of the PDF to approximate. The cumulants of a given random variable can be obtained analytically from its moments, which involve integrals of powers of the random variable [31]. For this reason, a stochastic Galerkin method (SGM) with global polynomials is employed for the solution of the SPDE. With this choice, the QoI is a polynomial function in the stochastic variable, so exact moments can be computed with appropriate quadrature rules. Hence, also the coefficients of the GC and ED expansions can be computed exactly. Another advantage of using the SGM is that, similar to [34] and [33], once the solution of the SPDE is obtained, realizations of the QoI can be obtained at almost

*Department of Scientific Computing, Florida State University, Tallahassee, FL 32306-4120, USA

[†]The London School of Economics and Political Science, London WC2A 2AE, UK

⁰**Funding:** MG and HW would like to thank the Isaac Newton Institute for Mathematical Sciences, Cambridge, for support and hospitality during the program *Uncertainty quantification for complex systems: theory and methodologies* where work on this paper was undertaken. This work was supported by UK EPSRC grant numbers EP/K032208/1 and EP/R014604/1. GC and MG were supported in part by the US Air Force Office of Scientific Research grant FA9550-15-1-0001 and by the US Department of Energy Office of Science grant DE-SC0016591.

no cost by means of Monte Carlo sampling, without having to compute the solution of the problem for each sample. The SGM is validated against the Monte Carlo method (MCM) for small input variances of the random data. The method we propose still makes use of the histogram to determine the PDF of the QoI, although the histogram is used only as a reference to determine the most appropriate truncation order of the series. Since the approximate PDF is given analytically as a truncated series, it does not depend directly on the histogram and so it is not affected by the dimension of the bins used to construct it. Moreover, the use of analytic formulas makes the computation of the PDF extremely fast.

The paper is structured as follows: in Section 2, the mathematical problem and the input data description are introduced; in Section 3, the two SFEMs employed for the solution of the SPDEs are described, namely the Monte Carlo method and the Stochastic Galerkin method; the theory on the Gram-Charlier and Edgeworth expansions is laid out in Section 4. Arguments on asymptotic expansions and convergence are given in Section 5 and Section 6, respectively. Numerical results are reported in Section 7, for different types of output distributions. The paper is concluded with Section 8, where our findings are discussed.

2 Formulation of the problem

For SPDEs, the stochasticity is taken into account assuming that the input data depends on a random variable, other than the physical variable as in standard partial differential equations [49, 14, 39, 52, 38, 51]. The input data consists of coefficient functions and forcing term. For simplicity, here it is assumed that the stochastic contribution is introduced only by the coefficients and not by the forcing term. The model SPDE considered is the Poisson problem defined on $D \times \Omega$, where $D \subset \mathbb{R}^d$ and Ω is the sample space

$$\begin{cases} -\nabla \cdot (a(\mathbf{x}, \omega) \nabla u(\mathbf{x}, \omega)) = f(\mathbf{x}) & \text{in } D \times \Omega \\ u(\mathbf{x}, \omega) = 0 & \text{on } \partial D \times \Omega. \end{cases} \quad (1)$$

As in [26, 3, 39, 38], the following assumption is made.

Assumption 1 *The coefficient function $a(\mathbf{x}, \omega)$ in system (1) has the following properties:*

1. *There exists $a_{\min} > -\infty$ and $a_{\max} < \infty$ such that $a_{\min} \leq a(\mathbf{x}, \omega) \leq a_{\max}$ almost surely on Ω , for all $\mathbf{x} \in D$.*
2. *$a(\mathbf{x}, \omega) = a(\mathbf{x}, \mathbf{y}(\omega))$ in $\bar{D} \times \Omega$, where $\mathbf{y}(\omega) = (y_1(\omega), y_2(\omega), \dots, y_N(\omega))$ is a vector of real-valued uncorrelated random variables defined on a probability space $(\Omega, \mathcal{F}, \mathbb{P})$.*
3. *$a(\mathbf{x}, \mathbf{y}(\omega))$ is measurable with respect to \mathbf{y} .*

For any $n = 1, \dots, N$, let $\Gamma_n \equiv y_n(\Omega) \subset \mathbb{R}$ and let us define the parameter space $\Gamma \equiv \prod_{n=1}^N \Gamma_n$. The joint probability density function (PDF) for $\{y_n\}_{n=1}^N$ is denoted by $\rho(\mathbf{y}) : \Gamma \rightarrow \mathbb{R}^+$. Several choices of coefficient functions are possible to ensure that Assumption 1 is satisfied. Some examples are given in [26]. The choice made in this work is described in the next section.

2.1 Karhunen-Loève Expansion

The Karhunen-Loève (KL) series expansion has been widely used in the field of uncertainty quantification to represent random fields, such as the coefficient function in system (1), as an infinite sum of random variables [32, 47, 24]. For numerical simulations, due to the finite computational capability available, the series is truncated, resulting in the following approximation

$$a(\mathbf{x}, \mathbf{y}(\omega)) \approx \mathbb{E}[a(\mathbf{x}, \cdot)] + \sum_{n=1}^N \sqrt{\lambda_n} b_n(\mathbf{x}) y_n(\omega), \quad (2)$$

where, for $n = 1, \dots, N$, λ_n and b_n are, respectively, the eigenvalues and eigenfunctions of the covariance function of $a(\mathbf{x}, \mathbf{y}(\omega))$ and the $\{y_n(\omega)\}_{n=1}^N$ are uncorrelated real-valued random variables.

Remark 1 *We assume that the input random processes approximated with a truncated KL expansion are Gaussian, hence the random variables $\{y_n(\omega)\}_{n=1}^N$ are standard independent and identically distributed. This allows us to generate realizations of the truncated KL expansion by Monte Carlo sampling from Gaussian distributions.*

To bound the coefficient function away from zero, the KL expansion is used on the logarithm of $a(\mathbf{x}, \mathbf{y}(\omega)) - a_{\min}$ rather than on the function itself. Thus, let us define the function $\gamma(\mathbf{x}, \mathbf{y}(\omega))$ as follows

$$\gamma(\mathbf{x}, \mathbf{y}(\omega)) \equiv \log(a(\mathbf{x}, \omega) - a_{\min}). \quad (3)$$

The above definition implies that

$$a(\mathbf{x}, \mathbf{y}(\omega)) = a_{\min} + \exp\left(\gamma(\mathbf{x}, \mathbf{y}(\omega))\right). \quad (4)$$

Using a truncated KL expansion to approximate $\gamma(\mathbf{x}, \mathbf{y}(\omega))$, we get

$$\gamma(\mathbf{x}, \mathbf{y}(\omega)) \approx \mu_\gamma + \sum_{n=1}^N \sqrt{\lambda_n} b_n(\mathbf{x}) y_n(\omega), \quad (5)$$

where $\mu_\gamma \equiv \mathbb{E}[\gamma(\mathbf{x}, \omega)]$, and N is the dimension of Γ . Note that, in Eq. (5), (λ_n, b_n) are the eigenpairs associated with the covariance function of $\gamma(\mathbf{x}, \mathbf{y}(\omega))$. Moreover, according to Remark 1, when the truncated KL is used to approximate $\gamma(\mathbf{x}, \mathbf{y}(\omega))$, the assumption of Gaussian distribution is made on $\gamma(\mathbf{x}, \mathbf{y}(\omega))$, and consequently $a(\mathbf{x}, \mathbf{y}(\omega))$ has a log-normal distribution, as shown in Eq. (4). It follows from Eq. (4) that $a(\mathbf{x}, \mathbf{y}(\omega))$ is approximated by

$$a(\mathbf{x}, \mathbf{y}(\omega)) \approx a_{\min} + \exp\left(\mu_\gamma + \sum_{n=1}^N \sqrt{\lambda_n} b_n(\mathbf{x}) y_n(\omega)\right). \quad (6)$$

The eigenvalues and eigenfunctions in Eq. (6) are obtained solving the generalized eigenvalue problem

$$\int_D C_\gamma(\mathbf{x}, \widehat{\mathbf{x}}) b_n(\mathbf{x}) d\mathbf{x} = \lambda_n b_n(\widehat{\mathbf{x}}), \quad (7)$$

where $C_\gamma(\mathbf{x}, \widehat{\mathbf{x}})$ is the covariance function of the field $\gamma(\mathbf{x}, \mathbf{y}(\omega))$. The covariance structure is generally unknown and usually a specific covariance function is assumed. In this work, the covariance function of $\gamma(\mathbf{x}, \mathbf{y}(\omega))$ is assumed to be

$$C_\gamma(\mathbf{x}, \widehat{\mathbf{x}}) = \sigma_\gamma^2 \exp\left[-\frac{1}{L} \left(\sum_{i=1}^d |x_i - \widehat{x}_i|\right)\right], \quad (8)$$

where σ_γ denotes the standard deviation of $\gamma(\mathbf{x}, \mathbf{y}(\omega))$, d is the dimension of the spatial variable and $L > 0$ is a correlation length which satisfies $L \leq \text{diam}(D)$.

The SPDE in Eq. (1) is solved using stochastic finite element (SFEM) methods, and the solution of Eq. (7) is obtained according to a Galerkin approach, following the procedure presented, for instance, in [47, 28]. Assume that the physical domain D is discretized with a regular finite element grid \mathcal{T}_h of size h [13, 10, 2], and let J_h be the total number of degrees of freedom. If $\{\phi_j\}_{j=1}^{J_h}$ denotes the global nodal basis associated with \mathcal{T}_h , the eigenfunction b_n of the covariance function of $\gamma(\mathbf{x}, \mathbf{y}(\omega))$ in Eq. (6) is approximated by its nodal interpolant

$$b_n(\mathbf{x}) \approx \sum_{j=1}^{J_h} b_{j,n} \phi_j(\mathbf{x}), \quad (9)$$

where $b_{j,n} \equiv b_n(\mathbf{x}_j)$, with \mathbf{x}_j being the j -th node of \mathcal{T}_h . A substitution of Eq. (9) in Eq. (7) transforms the continuous problem into a finite dimensional one

$$\sum_{j=1}^{J_h} b_{j,n} \left(\int_D C_\gamma(\mathbf{x}, \widehat{\mathbf{x}}) \phi_j(\mathbf{x}) d\mathbf{x} - \lambda_n \phi_j(\widehat{\mathbf{x}}) \right) = 0. \quad (10)$$

Next, Eq. (10) is multiplied by ϕ_i , and integrated with respect to $\widehat{\mathbf{x}}$, to obtain

$$\sum_{j=1}^{J_h} b_{j,n} \left(\int_D \int_D C_\gamma(\mathbf{x}, \widehat{\mathbf{x}}) \phi_j(\mathbf{x}) \phi_i(\widehat{\mathbf{x}}) d\mathbf{x} d\widehat{\mathbf{x}} - \lambda_n \int_D \phi_j(\widehat{\mathbf{x}}) \phi_i(\widehat{\mathbf{x}}) d\widehat{\mathbf{x}} \right) = 0. \quad (11)$$

Let us define the two real symmetric $J_h \times J_h$ matrices \mathbf{C} and \mathbf{M} by

$$C_{ij} \equiv \int_D \int_D C_\gamma(\mathbf{x}, \widehat{\mathbf{x}}) \phi_j(\mathbf{x}) \phi_i(\widehat{\mathbf{x}}) d\mathbf{x} d\widehat{\mathbf{x}}, \quad M_{ij} \equiv \int_D \phi_j(\widehat{\mathbf{x}}) \phi_i(\widehat{\mathbf{x}}) d\widehat{\mathbf{x}}. \quad (12)$$

Note that \mathbf{M} is the standard finite element mass matrix, and is positive definite. With these matrices, Eq. (11) can be rewritten as the vector equation

$$\mathbf{C}\mathbf{b}_n = \lambda_n \mathbf{M}\mathbf{b}_n, \quad (13)$$

Since \mathbf{C} is symmetric, its eigenvectors \mathbf{b}_n associated with distinct eigenvalues are orthogonal with respect to the mass matrix \mathbf{M} , that is $\mathbf{b}_n^T \mathbf{M} \mathbf{b}_m = 0$ if $m \neq n$. This orthogonality property implies that the approximations of the functions $b_n(\mathbf{x})$ in Eq. (9) are orthogonal in $L^2(D)$. Orthonormality can be obtained dividing these functions by their $L^2(D)$ norm. Note that orthonormality in $L^2(D)$ is a requirement for the functions $b_n(\mathbf{x})$.

For the numerical tests, the generalized eigenvalue problem in Eq. (13) is implemented in the in-house finite element code FEMuS [1], and solved with the SLEPc library [27].

2.2 Quantities of Interest

The aim is to approximate probability density functions of functionals of the SPDE solution, which we refer to as quantities of interest. Let $u_{J_h}(\mathbf{x}, \mathbf{y})$ be the approximate solution of system (1), obtained with an SFEM. The methods used to solve such a system are discussed in the next section. Given $u_{J_h}(\mathbf{x}, \mathbf{y})$, examples of quantities of interest include the spatial average over the physical domain

$$\mathcal{Q}_u(\mathbf{y}) = \frac{1}{|D|} \int_D u_{J_h}(\mathbf{x}, \mathbf{y}) d\mathbf{x}, \quad (14)$$

the integral of the square

$$\mathcal{Q}_u(\mathbf{y}) = \int_D \left(u_{J_h}(\mathbf{x}, \mathbf{y}) \right)^2 d\mathbf{x}, \quad (15)$$

or the maximum over the physical domain

$$\mathcal{Q}_u(\mathbf{y}) = \max_{\mathbf{x} \in D} u_{J_h}(\mathbf{x}, \mathbf{y}). \quad (16)$$

Note that the dependence on the physical variable \mathbf{x} is eliminated in the quantities of interest, as $\mathcal{Q}_u(\mathbf{y})$ is a scalar function that only depends on the stochastic variable \mathbf{y} .

3 Solution of the SPDE

The SPDE (1) is solved numerically using stochastic finite element methods. A detailed description of SFEMs for SPDEs with random input data such as the one in system (1) can be found in the review article [26] and references therein. The SFEM used here are described in the next two sections, together with the procedures to compute stochastic quantities such as moments, once the approximate SFEM solution is obtained.

3.1 The Monte Carlo Method

The first SFEM considered is the classical Monte Carlo Method (MCM), which is a stochastic sampling method [26]. With MCM, M points $\{\mathbf{y}_m\}_{m=1}^M$ are chosen randomly in the parameter domain Γ , and system (1) is solved independently for each of these points. In such a way, M realization of the solution of the SPDE are obtained and M uncoupled finite element systems are solved. For more details on MCM and error estimates, see [23, 35, 26]. From now on, the number M will be referred to as the number of MCM samples. According to Remark 1, the MCM samples are randomly drawn from Gaussian distributions. The mean μ_γ and standard deviation σ_γ of $\gamma(\mathbf{x}, \mathbf{y}(\omega))$ in Eq. (3) are not in general zero and one, respectively. Hence, if one chooses samples for the KL expansion from a standard Gaussian distribution, because of the presence of μ_γ in the KL and σ_γ in the covariance function, the result is the same as sampling from a non-standard Gaussian distribution with mean μ_γ and standard deviation σ_γ . If \mathbf{y}_m denotes one of the M samples obtained from the Monte Carlo Method, let $u_{J_h}(\mathbf{x}, \mathbf{y}_m)$ be the MCM solution of system (1) associated with the sample \mathbf{y}_m and let $\mathcal{Q}_u(\mathbf{y}_m)$ be a value of a quantity of interest obtained from the realization $u_{J_h}(\mathbf{x}, \mathbf{y}_m)$. Then $\mathcal{Q}_u(\mathbf{y}_m)$ is not a function of a random variable but rather just a scalar quantity. On the other hand, the quantity of interest $\mathcal{Q}_u(\mathbf{y})$ is a function of a random variable, and a random variable itself. Hence stochastic quantities such as moments and cumulants can be

computed. In the framework of MCM, the mean of $\mathcal{Q}_u(\mathbf{y})$ is approximated with Monte Carlo integration as follows

$$\mathbb{E}[\mathcal{Q}_u(\mathbf{y})] \approx \frac{1}{M} \sum_{m=1}^M \mathcal{Q}_u(\mathbf{y}_m) \equiv \mu_{\mathcal{Q}_u}. \quad (17)$$

For $l > 1$, the l -th moment is approximated in the same fashion by

$$\mathbb{E}[(\mathcal{Q}_u(\mathbf{y}))^l] \approx \frac{1}{M} \sum_{m=1}^M (\mathcal{Q}_u(\mathbf{y}_m))^l. \quad (18)$$

An estimate of the variance is given by

$$\mathbb{E}[(\mathcal{Q}_u(\mathbf{y}) - \mathbb{E}[\mathcal{Q}_u(\mathbf{y})])^2] \approx \frac{1}{M} \sum_{m=1}^M (\mathcal{Q}_u(\mathbf{y}_m) - \mu_{\mathcal{Q}_u})^2 \equiv \sigma_{\mathcal{Q}_u}^2.$$

The accuracy of Monte Carlo integration improves with the number of samples M , but the sampling error increases with the magnitude of the input variance [26]. For this reason, here the MCM is used only for small values of the input variance and to validate the stochastic Galerkin method, which is later employed for larger values of the input variance.

3.2 The Stochastic Galerkin Method

The second SFEM used to obtain an approximation of the solution of system (1) is a stochastic Galerkin method (SGM). With SGMs, the stochastic function space is approximated using a Galerkin procedure, as it is done for the physical function space in standard finite element methods [25, 4, 5]. Let us assume that the parameters are independent, so that the input joint probability function $\rho(\mathbf{y})$ can be expressed as $\rho(\mathbf{y}) = \prod_{n=1}^N \rho_n(y_n)$. According to a Galerkin methodology, the infinite dimensional space $L_\rho^2(\Gamma)$ is approximated by the finite dimensional space

$$\mathcal{P}_{\mathcal{J}(p)}(\Gamma) = \text{span} \left\{ \prod_{n=1}^N y_n^{p_n} \mid \mathbf{p} \in \mathcal{J}(p), y_n \in \Gamma_n \right\}, \quad (19)$$

where $\mathcal{J}(p) = \left\{ \mathbf{p} \in \mathbb{N}^N \mid \sum_{n=1}^N p_n \leq p \right\}$,

which corresponds to the total degree (TD) multivariate polynomial space from [26]. Gaussian PDFs are assumed for the input variables, hence the probabilist Hermite polynomials are employed as an orthogonal basis for $\mathcal{P}_{\mathcal{J}(p)}(\Gamma)$. Moreover, it holds that $\Gamma_n = \mathbb{R}$ for all $n = 1, \dots, N$, and so $\Gamma = \mathbb{R}^N$. The Hermite polynomials are appropriately scaled so that they form an orthonormal basis with respect to the PDF

$$\rho_n(y_n) = \frac{\exp(-y_n^2/2)}{\sqrt{2\pi}}. \quad (20)$$

The scaling is carried out by dividing the p_n -th probabilist Hermite polynomial $H_{e_{p_n}}$ by $\sqrt{n!}$, to obtain

$$\int_{\mathbb{R}} \frac{H_{e_{p_n}}}{\sqrt{n!}} \frac{H_{e_{p_m}}}{\sqrt{m!}} \rho_n(y_n) dy_n = \delta_{nm}, \quad (21)$$

where $\rho_n(y_n)$ is as in Eq. (20) and δ_{nm} is Kronecker's delta. Multivariate $L_\rho^2(\Gamma)$ -orthonormal Hermite polynomials are defined as tensor product of the univariate polynomials as

$$H_{e_{\mathbf{p}}}(\mathbf{y}) = \prod_{n=1}^N H_{e_{p_n}}(y_n). \quad (22)$$

The SGM approximation of the solution of system (1) is defined as [26]

$$u_{J_h M_p}^{gSG}(\mathbf{x}, \mathbf{y}) = \sum_{\mathbf{p} \in \mathcal{J}(p)} \sum_{j=1}^{J_h} u_{\mathbf{p}, j} \phi(\mathbf{x}) H_{e_{\mathbf{p}}}(\mathbf{y}).$$

Quantities of interests are now given by

$$\mathcal{Q}_u(\mathbf{y}) = \sum_{\mathbf{p} \in \mathcal{J}(p)} \beta_{\mathbf{p}} H_{e_{\mathbf{p}}}(\mathbf{y}), \quad (23)$$

where the value of $\beta_{\mathbf{p}}$ identifies different quantities of interest. For instance, if

$$\beta_{\mathbf{p}} = \frac{1}{|D|} \int_D \sum_{j=1}^{J_h} u_{\mathbf{p},j} \phi(\mathbf{x}) d\mathbf{x}, \quad (24)$$

then $\mathcal{Q}_u(\mathbf{y})$ in Eq. (23) is the average of the solution over the domain defined in Eq. (14), while if

$$\beta_{\mathbf{p}} = \int_D \left(\sum_{j=1}^{J_h} u_{\mathbf{p},j} \phi(\mathbf{x}) \right)^2 d\mathbf{x}, \quad (25)$$

then $\mathcal{Q}_u(\mathbf{y})$ is the integral of the square of the solution as in Eq. (15). As opposed to what it is obtained with MCM, the quantities of interest given by the SGM are now polynomial functions in the variable \mathbf{y} . Such a feature gives a considerable advantage in terms of accuracy, since moments can now be computed exactly with appropriate quadrature rules, rather than being approximated by Monte Carlo integration. The l -th moment of the $\mathcal{Q}_u(\mathbf{y})$ in Eq. (24) is defined as

$$\mathbb{E} \left[\left(\mathcal{Q}_u(\mathbf{y}) \right)^l \right] \equiv \int_{\mathbb{R}^N} \left(\mathcal{Q}_u(\mathbf{y}) \right)^l \rho(\mathbf{y}) d\mathbf{y}. \quad (26)$$

The multivariate integral in the above equation can be computed exactly with a multidimensional Hermite quadrature rule. Exploiting Eq. (21), unidimensional quadrature points can be obtained as the zeros of the probabilist Hermite polynomials. The quadrature weights are given by the following formula

$$w_i = \frac{(n-1)!}{n (H_{e_{n-1}}(x_i))^2}, \quad (27)$$

where x_i is the i -th quadrature point and $H_{e_{n-1}}$ is the $(n-1)$ -th probabilist Hermite polynomial. By construction, the weights w_i have the property that $\sum_i^{N_q} w_i = 1$, where N_q is the total number of quadrature points employed in the data projection. Multidimensional quadrature points and weights can be obtained in a tensor product fashion. For the SGM, given $q \in \mathbb{N}$, the coefficient function $a(\mathbf{x}, \mathbf{y})$ in system (1) is computed as [26]

$$\begin{aligned} a_{SGM}(\mathbf{x}, \mathbf{y}) &= \sum_{\mathbf{q} \in \mathcal{J}(q)} a_{\mathbf{q}}(\mathbf{x}) H_{e_{\mathbf{q}}}(\mathbf{y}), \\ a_{\mathbf{q}}(\mathbf{x}) &= \int_{\Gamma} a(\mathbf{x}, \mathbf{y}(\omega)) H_{e_{\mathbf{q}}}(\mathbf{y}) \rho(\mathbf{y}) d\mathbf{y}, \end{aligned} \quad (28)$$

with $a(\mathbf{x}, \mathbf{y}(\omega))$ as in Eq. (4). In the numerical results, with the exception of the integral for the data projection in Eq. (28), all other integrals are computed by an exact quadrature rule. Among the integrals that are computed exactly, there are also the moments in Eq. (26). It is worth mentioning that, if a non-standard Gaussian distribution with mean μ_{γ} and standard deviation σ_{γ} is considered for the input variables, the change of variable $(x - \mu_{\gamma})/\sigma_{\gamma}$ would have to be made in all integrals over the parameter space. Although, one can avoid this change of variable by taking into account the non-standard distribution in the input data, as it has been discussed in Section 3.1.

4 The Gram-Charlier and Edgeworth expansions

The goal of this paper is to obtain the PDF $f_{\mathcal{Q}_u} : \mathbb{R} \rightarrow \mathbb{R}^+$ of a given quantity of interest $\mathcal{Q}_u(\mathbf{y})$ using the Gram-Charlier (GC) and the Edgeworth (ED) series expansions, which express the PDF in terms of a reference PDF. The coefficients of these expansions are functions of the cumulants of $\mathcal{Q}_u(\mathbf{y})$, which can be easily obtained once the moments of $\mathcal{Q}_u(\mathbf{y})$ have been computed. In general, if we denote by m_l and κ_l the l -th moment and the l -th cumulant respectively, the first six cumulants are expressed in terms of

the moments as follows [31, 7]:

$$\begin{aligned}
\kappa_1 &= m_1, \\
\kappa_2 &= m_2 - m_1^2, \\
\kappa_3 &= m_3 + 2m_1^3 - 3m_1 m_2, \\
\kappa_4 &= m_4 - 6m_1^4 + 12m_1^2 m_2 - 3m_2^2 - 4m_1 m_3, \\
\kappa_5 &= m_5 - 5m_4 m_1 - 10m_3 m_2 + 20m_3 m_1^2 + 30m_2^2 m_1 - 60m_2 m_1^3 + 24m_1^5, \\
\kappa_6 &= m_6 - 6m_5 m_1 - 15m_4 m_2 + 30m_4 m_1^2 - 10m_3^2 + 120m_3 m_2 m_1 \\
&\quad - 120m_3 m_1^3 + 30m_2^3 - 270m_2^2 m_1^2 + 360m_2 m_1^4 - 120m_1^6.
\end{aligned} \tag{29}$$

In practical applications, the GC and ED series are truncated and only a finite number of terms is retained. The truncation results in an approximation of the PDF $f_{\mathcal{Q}_u}$. The behavior of the truncated series as the number of terms is increased will be subject to a discussion in the next sections.

4.1 Derivation of the expansions

We choose the formulation given in [9] to formally describe the GC and ED series. Let X be any random variable with PDF $f_X(x)$. The characteristic function $\Psi_X(t)$ of X is the Fourier transform of $f_X(x)$ [31]. The cumulant generating function $K(t)$ is defined as $K(t) \equiv \ln(\Psi_X(t))$, and it holds that

$$\ln(\Psi_X(t)) = \sum_{l=1}^{\infty} \kappa_{X,l} \frac{(it)^l}{l!}, \tag{30}$$

where i denotes the imaginary unit and $\kappa_{X,l}$ is the l -th cumulant of X . Let φ denote the standard Gaussian distribution defined in Eq. (20). With the same notation used for X , the following equation can be obtained

$$\ln(\Psi_{\varphi}(t)) = \sum_{l=1}^{\infty} \kappa_{\varphi,l} \frac{(it)^l}{l!}. \tag{31}$$

Using the properties of exponentials and convergent series, Eq. (30) and Eq. (31) can be combined to get

$$\Psi_X(t) = \exp\left(\sum_{l=1}^{\infty} (\kappa_{X,l} - \kappa_{\varphi,l}) \frac{(it)^l}{l!}\right) \Psi_{\varphi}(t). \tag{32}$$

The GC and ED expansions follow from different manipulations of Eq. (32).

The GC is obtained with the use of Bell polynomials $B_l(x_1, \dots, x_l)$ [6, 36]. These polynomials have the property that

$$\exp\left(\sum_{l=1}^{\infty} x_l \frac{(it)^l}{l!}\right) = \sum_{l=0}^{\infty} B_l(x_1, \dots, x_l) \frac{(it)^l}{l!}, \tag{33}$$

with $B_0 \equiv 1$. Therefore, Eq. (32) becomes

$$\Psi_X(t) = \left(1 + \sum_{l=1}^{\infty} B_l(\kappa_{X,1} - \kappa_{\varphi,1}, \dots, \kappa_{X,l} - \kappa_{\varphi,l}) \frac{(it)^l}{l!}\right) \Psi_{\varphi}(t). \tag{34}$$

The inverse Fourier transform applied to Eq. (34) gives the GC expansion

$$f_X(x) = \left(1 + \sum_{l=1}^{\infty} B_l(\kappa_{X,1} - \kappa_{\varphi,1}, \dots, \kappa_{X,l} - \kappa_{\varphi,l}) \frac{(-1)^l D_x^{(l)}}{l!}\right) \varphi(x), \tag{35}$$

where $D_x^{(l)}$ represents the l -th derivative operator with respect to x and

$$D_x^{(l)}(\varphi(x)) = (-1)^l H_{e_l}(x) \varphi(x). \tag{36}$$

The first six Bell polynomials are given by [9]

$$\begin{aligned}
B_1(x_1) &= x_1, \\
B_2(x_1, x_2) &= x_1^2 + x_2, \\
B_3(x_1, x_2, x_3) &= x_1^3 + 3x_1x_2 + x_3, \\
B_4(x_1, x_2, x_3, x_4) &= x_1^4 + 6x_1^2x_2 + 3x_2^2 + 4x_1x_3 + x_4, \\
B_5(x_1, x_2, x_3, x_4, x_5) &= x_1^5 + 10x_1^3x_2 + 15x_1x_2^2 + 10x_1^2x_3 + 10x_2x_3 + 5x_1x_4 + x_5, \\
B_6(x_1, x_2, x_3, x_4, x_5, x_6) &= x_1^6 + 15x_1^4x_2 + 45x_1^2x_2^2 + 15x_2^3 + 20x_1^3x_3 + 60x_1x_2x_3 \\
&\quad + 10x_3^2 + 15x_1^2x_4 + 15x_2x_4 + 6x_1x_5 + x_6.
\end{aligned} \tag{37}$$

Note that when X is a standardized variable, $\kappa_{X,0} = 0$ and $\kappa_{X,1} = 1$. Since $\kappa_{\varphi,0} = 0$, $\kappa_{\varphi,1} = 1$, and $\kappa_{\varphi,l} = 0$ for $l \geq 3$, Eq. (35) reduces to

$$f_X(x) = \left(1 + \sum_{l=3}^{\infty} B_l(0, 0, \kappa_{X,3}, \dots, \kappa_{X,l}) \frac{(-1)^l D_x^{(l)}}{l!}\right) \varphi(x), \tag{38}$$

To derive ED, one assumes that X can be written as the standardized sum [43, 44]

$$X = \frac{1}{\sqrt{r}} \sum_{i=1}^r \frac{Z_i - \mu}{\sigma}, \tag{39}$$

where the random variables Z_1, Z_2, \dots, Z_r are independent and identically distributed, each with mean μ , standard deviation σ , and l -th cumulant $\kappa_{Z,l}$. Note that $\kappa_{Z,1} = \mu$ and $\kappa_{Z,2} = \sigma^2$. Define $\nu_l = \kappa_{Z,l}/\sigma^l$, then [9]

$$\kappa_{X,0} = 0, \quad \kappa_{X,1} = 1, \quad \kappa_{X,l} = \frac{\nu_l}{r^{\frac{l}{2}-1}}, \quad l \geq 3. \tag{40}$$

Substituting the above equation in Eq. (32), we get

$$\Psi_X(t) = \exp\left(\sum_{l=3}^{\infty} \frac{\nu_l}{r^{\frac{l}{2}-1}} \frac{(it)^l}{l!}\right) \Psi_{\varphi}(t). \tag{41}$$

With a proper shift of the summation index and an inverse Fourier transform, the above series gives the ED expansion

$$f_X(x) = \left(1 + \sum_{l=1}^{\infty} B_l(a_1, a_2, \dots, a_l) \frac{1}{r^{l/2} l!}\right) \varphi(x), \tag{42}$$

The interested reader can consult [9] for more details on how the above equation is obtained. The coefficients a_l are given by

$$a_l = \frac{\nu_{l+2} (-1)^{l+2} D_x^{(l+2)}}{(l+1)(l+2)}. \tag{43}$$

For ease of notation, if we write the series in Eq. (42) as

$$f_X(x) = \sum_{l=0}^{\infty} (-1)^l \frac{\vartheta_l(x)}{r^{l/2}}, \tag{44}$$

the first six coefficient functions $\vartheta_l(x)$ are given by [8]

$$\begin{aligned}
\vartheta_0(x) &= \varphi(x), \\
\vartheta_1(x) &= \frac{1}{3!} \nu_3 D_x^{(3)}(\varphi(x)), \\
\vartheta_2(x) &= \frac{1}{4!} \nu_4 D_x^{(4)}(\varphi(x)) + \frac{1}{72} \nu_3^2 D_x^{(6)}(\varphi(x)), \\
\vartheta_3(x) &= \frac{1}{5!} \nu_5 D_x^{(5)}(\varphi(x)) + \frac{1}{144} \nu_3 \nu_4 D_x^{(7)}(\varphi(x)) + \frac{1}{1296} \nu_3^3 D_x^{(9)}(\varphi(x)), \\
\vartheta_4(x) &= \frac{1}{6!} \nu_6 D_x^{(6)}(\varphi(x)) + \left(\frac{1}{1152} \nu_4^2 + \frac{1}{720} \nu_3 \nu_5\right) D_x^{(8)}(\varphi(x)) \\
&\quad + \frac{1}{1728} \nu_3^2 \nu_4 D_x^{(10)}(\varphi(x)) + \frac{1}{31104} \nu_3^4 D_x^{(12)}(\varphi(x)).
\end{aligned} \tag{45}$$

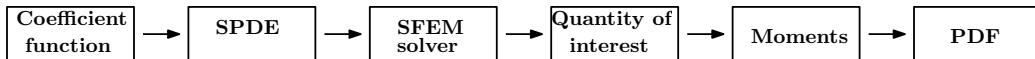


Figure 1: Summary of the steps to obtain an approximation of the PDF f_{Q_u} .

A schematic representation of the necessary steps to get from the coefficient function $a(\mathbf{x}, \mathbf{y}(\omega))$ to the approximation of the PDF f_{Q_u} is summarized in Figure 1. Referring to Figure 1, the physical variable \mathbf{x} and the stochastic variable \mathbf{y} are given as inputs to the coefficient function $a(\mathbf{x}, \mathbf{y}(\omega))$, which is used to assemble the SFEM system associated with the SPDE in (1). The system is then solved with an SFEM and an approximate solution is obtained. From this solution, quantities of interest are evaluated and their moments are computed, in the way associated with the SFEM chosen. Once the moments have been obtained, they are fed to the truncated series expansions described in this section and an approximation of the PDF f_{Q_u} is produced. In the next two sections, important considerations on the convergence of the GC and ED expansions are made. First, the concept of asymptotic expansion is discussed.

5 Asymptotic expansions

Let $\{F_n(x)\}$ be a sequence of functions to be approximated by any partial sum of the series

$$\sum_{i=0}^{\infty} \frac{A_i(x)}{(\sqrt{n})^i}. \quad (46)$$

According to Wallace [50], for a given n , the series (46) is an asymptotic expansion valid to r terms if the first $r + 1$ partial sums have the property

$$\left| F_n(x) - \sum_{i=0}^r \frac{A_i(x)}{(\sqrt{n})^i} \right| \leq \frac{C_r(x)}{(\sqrt{n})^{r+1}}. \quad (47)$$

Moreover, if $C_r(x)$ does not depend on x , the expansion is said to be valid uniformly in x . As pointed out by Wallace, the asymptotic property is a property of finite partial sums and, for a given n , the series (46) may or may not be convergent. If the series (46) converges to F_n , we know that for every $\varepsilon > 0$ there is an $R \in \mathbb{N}$ such that

$$\left| F_n(x) - \sum_{i=0}^r \frac{A_i(x)}{(\sqrt{n})^i} \right| < \varepsilon, \quad \forall r \geq R. \quad (48)$$

While the above inequality states that for all partial sums with $r \geq R$, the error will be less than ε , it does not give specific information of what happens to the error before r reaches R . On the other hand, if n is sufficiently large, an asymptotic expansion valid to r terms has the property that the error will be uniformly reduced as more terms are added to the finite partial sum, from 1 up to $r + 1$ terms, after which there is no longer the guarantee that adding successive terms will provide a uniform reduction of the error [50]. With small n , the situation is a little different. Since the bounds $C_r(x)$ increase rapidly with r , a small value of n may be unable to make the denominator grow faster than the numerator of the right hand side in Ineq. 47, and typically only the first few terms are improvements, as pointed out by Wallace [50]. If a series is convergent, regardless of it being also asymptotic, the error will eventually go to zero as the number of terms in the partial sums is increased. If a series is asymptotic but not convergent, regardless of the value of n , there will be a minimum error that can be achieved, which limits the accuracy of the series. To summarize: convergent series give information on what happens to the error as the number of terms in the partial sum goes to infinity, while asymptotic series give information on the error as more terms are added starting from the first, and up to the $(r + 1)$ -th term.

6 Considerations on convergence

In [31] (page 152), the following sufficient condition for the convergence of the GC expansion is given

Proposition 1 *If the PDF $f(x)$ is of bounded variation on every finite interval and*

$$\int_{-\infty}^{\infty} |f(x)| \exp(-x^2/4) dx < \infty, \quad (49)$$

then the GC expansion of $f(x)$ is convergent.

While the integral in Proposition 1 is finite for PDFs with bounded support, the requirement of being of bounded variations on every finite interval is in general harder to satisfy. We could not find in the literature any explicit sufficient condition addressing the convergence of the Edgeworth (ED) expansion.

Although, as pointed out by several authors [31, 17, 37, 22], convergence of the GC or ED series should not be a concern, since for practical applications the series are truncated. Of course, if the series are convergent, the error will eventually go to zero, but this is not useful for practical applications since the number of terms necessary to achieve convergence will likely be too big. The real question is how well a truncated GC or ED series can approximate the PDF of interest. This is directly connected to the definition of asymptotic expansion introduced in the previous section. With an asymptotic expansion, there is the guarantee that the initial error will be reduced by adding a certain number of successive terms. This property is relevant for our purpose regardless of the convergence of the series, since only a finite number of terms after the initial approximation are considered. Unfortunately, the GC series is not an asymptotic expansion [50, 8, 42, 30]. On the other hand, it has been shown in [16] that the ED expansion is asymptotic uniformly in x . Even though explicit bounds on errors were not given in [16], the asymptotic nature of ED expansion still makes it more valuable than the GC for the applications of our interest, where the series are truncated to a small number of terms.

In light of these observations, we believe that the best approach is composed of two steps:

1. Run a Monte Carlo simulation to obtain the histogram. In this way a first approximation of the PDF is obtained, together with the bounds on the quantity of interest, in case it is bounded. Note that with SGM, once the quantity of interest has been obtained, Monte Carlo sampling can be done without the solution of any SPDE so a large number of samples can be produced, at almost no cost.
2. Compute the ED and GC expansions considering a number of terms decided a priori and determine if there is a curve that provides a good approximation of the histogram. Monitoring the error in the Edgeworth expansion, one can have information on the quality of the approximation.

Numerical results are reported in the next section, following the above two step scheme.

7 Numerical Results

We consider random variables associated with the solution of (1), obtained with the SFEMs discussed above. The methods are implemented in the in-house C++ FEM solver FEMuS [1], while the generalized eigenvalue problem in Eq. (13) is solved with the SLEPc library [27]. All numerical tests consider $f \equiv 1$ and dimension $d = 2$, for simplicity. The physical domain D is a unit square, with coarse grid composed of four bi-quadratic quadrilateral elements. The mesh for the simulations is obtained by refining three times the coarse grid according to a midpoint refinement procedure. The random field $a(\mathbf{x}, \mathbf{y}(\omega))$ is given by Eq. (6), and it is assumed that $\mu_\gamma = 0$. We chose $a_{\min} = 1/100$, and $L = 0.1$ for the covariance function in Eq. (8). The stochastic dimension is $N = 2$. The input standard deviation σ_γ is varied during the simulations. The quantities of interest are the average of the solution over the physical domain (14), and the integral of the square of the solution (15). For MCM, the number of samples is $M = 100000$. The same amount of samples is used to obtain the histograms, with both MCM and SGM. The one associated with SGM is obtained sampling random values of \mathbf{y} from a standard Gaussian distribution and plugging them in Eq. (23), once the SGM system has been solved. This allows to have a large number of realizations at almost no cost, as opposed to the MCM that solves the SPDE for each sample. For SGM, we choose the values of $p = 4$ in Eq. (19), and $q = 5$ in Eq. (28).

Remark 2 *When using GC, the quantity of interest is standardized before computing the moments, so the expansion adopted for the tests is Eq. (38). For ED, considering Eq. (42), it is assumed that $r = 1$ and that $Z_1 = Q_u$. Hence, for both the GC and the ED expansions, the PDF refers to the standardized quantity of interest.*

7.1 Tests with nearly Gaussian output distribution

We begin with simulations where the output distribution of the quantity of interest is close to a standard Gaussian. For the average of the solution over the domain, this is achieved with $\sigma_\gamma \in \{0.02, 0.04, 0.06, 0.08\}$. Since the truncated GC and ED expansions perform successive corrections of a standard Gaussian distribution as more terms are retained, it is expected that the expansions will perform very well in this context. In Figure 2, the eigenfunctions $b_1(\mathbf{x})$ and $b_2(\mathbf{x})$ from Eq. (6) are reported for $\sigma_\gamma = 0.08$. The values of the moments and cumulants for the average of the solution over the physical domain are shown in Table 1. Note that such values are associated with the non-standardized quantity of interest. As

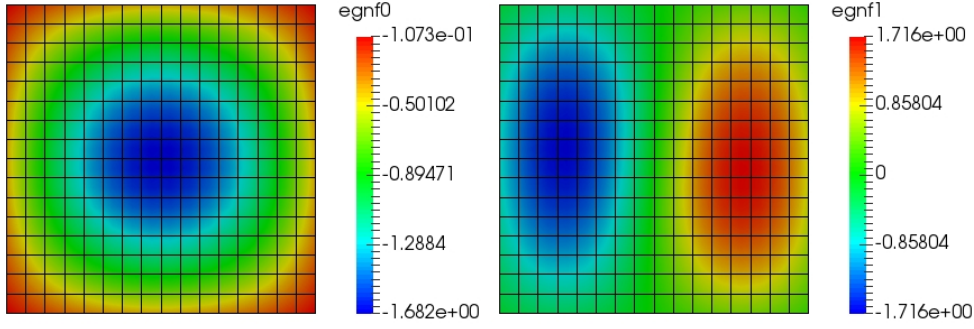


Figure 2: First eigenfunction (left) and second eigenfunction (right) in the KL expansion from Eq. (6) for the case of $\sigma_\gamma = 0.08$ and $N = 2$.

SFEM	Spatial Average ($N = 2$)					
	$\sigma_\gamma = 0.08$					
	m_1	m_2	m_3	m_4	m_5	m_6
MCM	-3.47977e-2	1.21102e-3	-4.21507e-5	1.46726e-6	-5.10815e-8	1.77857e-9
SGM	-3.47917e-2	1.21047e-3	-4.21150e-5	1.46528e-6	-5.09813e-8	1.77379e-9
	κ_1	κ_2	κ_3	κ_4	κ_5	κ_6
MCM	-3.47977e-2	1.42457e-7	0	0	0	0
SGM	-3.47917e-2	8.49990e-8	0	0	0	0
	$\sigma_\gamma = 0.06$					
	m_1	m_2	m_3	m_4	m_5	m_6
MCM	-3.47969e-2	1.21090e-3	-4.21415e-5	1.46668e-6	-5.10498e-8	1.77697e-9
SGM	-3.47936e-2	1.21060e-3	-4.21216e-5	1.46558e-6	-5.09937e-8	1.77430e-9
	κ_1	κ_2	κ_3	κ_4	κ_5	κ_6
MCM	-3.47969e-2	8.01228e-8	0	0	0	0
SGM	-3.47936e-2	4.77798e-9	0	0	0	0
	$\sigma_\gamma = 0.04$					
	m_1	m_2	m_3	m_4	m_5	m_6
MCM	-3.47964e-2	1.21082e-3	-4.21350e-5	1.46627e-6	-5.10273e-8	1.77583e-9
SGM	-3.47950e-2	1.21069e-3	-4.21263e-5	1.46579e-6	-5.10026e-8	1.77466e-9
	κ_1	κ_2	κ_3	κ_4	κ_5	κ_6
MCM	-3.47964e-2	3.56071e-8	0	0	0	0
SGM	-3.47950e-2	2.12252e-9	0	0	0	0
	$\sigma_\gamma = 0.02$					
	m_1	m_2	m_3	m_4	m_5	m_6
MCM	-3.47961e-2	1.21078e-3	-4.21312e-5	1.46603e-6	-5.10140e-8	1.77516e-9
SGM	-3.47958e-2	1.21075e-3	-4.21291e-5	1.46592e-6	-5.10080e-8	1.77487e-9
	κ_1	κ_2	κ_3	κ_4	κ_5	κ_6
MCM	-3.47961e-2	8.90134e-9	0	0	0	0
SGM	-3.47958e-2	5.30470e-10	0	0	0	0

Table 1: Behavior of moments and cumulants of the spatial average for $\sigma_\gamma \in \{0.02, 0.04, 0.06, 0.08\}$.

discussed in [26], the sampling error of the MCM increases with the input standard deviation, hence we use this method only for small values of σ_γ , such as those considered in this section. The results obtained with MCM are relevant since they serve as a validation of the SGM, that is employed in the next section for general output distributions. Observing Table 1, it is fair to say that convergence has been reached for the moments, since there is a good agreement between the MCM and the SGM predictions. The largest difference between MCM and SGM moments occurs for $\sigma_\gamma = 0.08$: it is of order 10^{-4} for the first two moments, of order 10^{-2} for the fifth moment, and of order 10^{-3} for the others. This means that the SGM can be considered validated by the MCM results. All cumulants κ_l with $l \geq 3$ are zero, confirming that the PDF is close to a Gaussian distribution, which is the one distribution that has $\kappa_l = 0$ for $l \geq 3$.

The histograms for $\sigma_\gamma = 0.08$ are in Figure (3). As expected, both suggest a nearly-Gaussian PDF, with the one for SGM just slightly more asymmetric with respect to the vertical axis. The major difference with an actual Gaussian distribution is that the histograms have bounded support. This is due to the

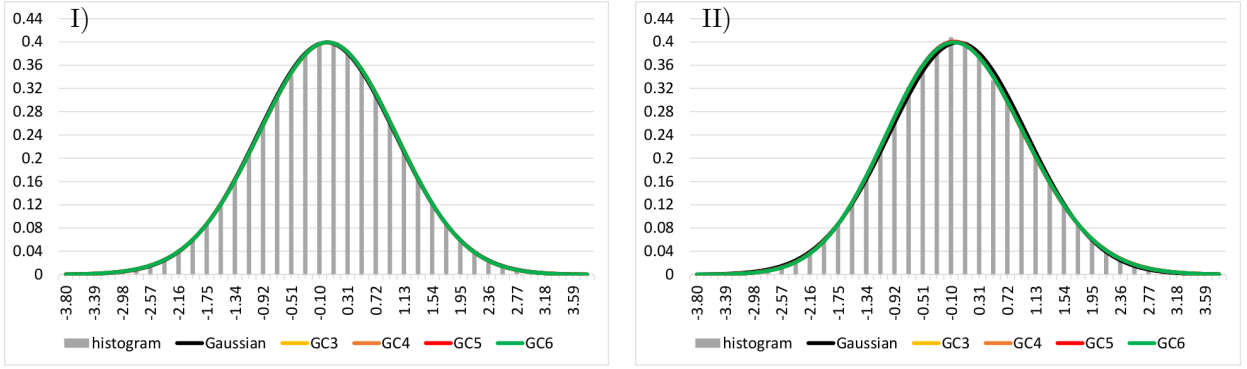


Figure 3: Gram-Charlier expansions of the standardized spatial average for $\sigma_\gamma = 0.08$ and $N = 2$. I): GC - MCM, II): GC - SGM.

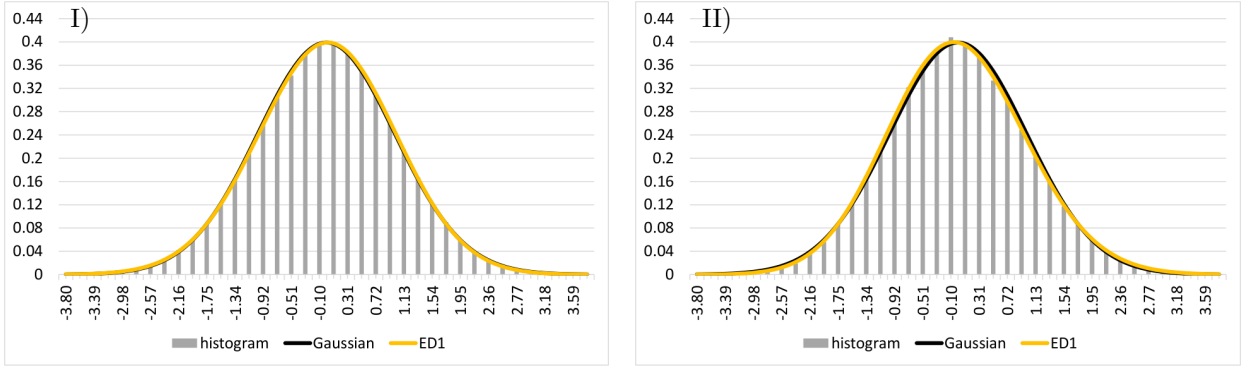


Figure 4: Edgeworth expansions of the standardized spatial average for $N = 2$ and $\sigma_\gamma = 0.08$. I): ED - MCM, II): ED - SGM.

fact that the quantity of interest is bounded. Our tests have shown that larger values of σ_γ cause an increased skewness on the histograms, although this effect is very weak for the values of σ_γ considered here, and so histograms for $\sigma_\gamma = 0.02, 0.04$ and 0.06 are not shown due to their strong similarity to those in Figure 3. The increased skewness will be clearly visible when larger values of σ_γ are considered in the next section.

In Figure 3, the truncated GC expansion is displayed for $\sigma_\gamma = 0.08$. GC expansions for other values of σ_γ have not been reported since they bear a strong resemblance to those in Figure 3. The notation GC_j means that the GC expansion in Eq. (38) has been truncated at $l = j$. Truncations up to $l = 6$ have been computed. The GC expansion is a polynomial function defined on all \mathbb{R} , hence it could be graphed for ideally any x . Although, after the range of values of the quantity of interest is obtained from the histogram, the graph of the GC is plotted only for values of x in such a range. The same is done for Edgeworth. Referring to Figure 3, we see that the GC expansions are in good agreement with the respective histogram. The GC curves for SGM even catch the slight positive skewness of the PDF.

In Figure 4 the truncated ED expansions are shown for MCM and SGM. Only the results for $\sigma_\gamma = 0.08$ are reported, since other values produced similar graphs. Note that, for GC, all computed truncated series are displayed in Figure 3, namely GC3, GC4, GC5 and GC6. As discussed above, GC is not an asymptotic expansion and so it might be the case that, for instance, GC4 is a worse approximation than GC3 but GC5 is better than both GC3 and GC4. Hence, it makes sense to display all computed curves, to have an idea of the behavior of the truncated series. For ED, truncations up to four terms have been computed. However, not all curves are displayed in the figures, but only those that show a monotone reduction of the error. Such curves are typically ED1 and ED2. This scenario is expected considering the discussion in Section 5, and that $r = 1$ in Eq. (39). Figure 4 shows great agreement of the ED expansion with the histograms, for both the MCM and the SGM.

When the distribution of the quantity of interest is nearly Gaussian, our results suggest that the Gram-Charlier and Edgeworth expansions can effectively be used to describe the PDF of the quantity of interest. This is consistent with the nature of such expansions, that add successive corrections to a standard Gaussian distribution. The natural question that arises next concerns how well GC and ED can work when the PDF to approximate is not nearly Gaussian. Numerical results are presented in the next section to address this uncertainty.

Standardized spatial average (SGM, $N = 2$)								
σ_γ	Moments				Cumulants			
	m_{3STD}	m_{4STD}	m_{5STD}	m_{6STD}	κ_{3STD}	κ_{4STD}	κ_{5STD}	κ_{6STD}
1	0.90682	3.79165	9.31739	33.8533	0.90682	0.79165	0.24916	-1.24479
0.8	0.82677	3.64985	8.31118	29.8763	0.82677	0.64985	0.04343	-1.70699
0.6	0.70532	3.48968	7.08384	26.2076	0.70532	0.48968	0.03057	-1.11248
0.4	0.52667	3.29185	5.31262	21.8085	0.52667	0.29185	0.04587	-0.34315

Table 2: Moments and cumulants of the standardized spatial average obtained with SGM and $N = 2$, for different values of the input standard deviation.

Standardized integral of the square (SGM, $N = 2$)								
σ_γ	Moments				Cumulants			
	m_{3STD}	m_{4STD}	m_{5STD}	m_{6STD}	κ_{3STD}	κ_{4STD}	κ_{5STD}	κ_{6STD}
1.15	1.91096	9.76845	56.4319	448.225	1.91096	6.76845	37.3222	295.180
1.10	0.92839	4.57980	13.3539	61.5390	0.92839	1.57980	4.06999	14.2227
1.05	0.43868	3.50985	5.22884	26.4527	0.43868	0.50985	0.84194	1.88051
1.00	0.35665	3.23984	3.81059	20.1986	0.35665	0.23984	0.24402	0.32893

Table 3: Moments and cumulants of the standardized integral of the square obtained with SGM and $N = 2$, for different values of the input standard deviation.

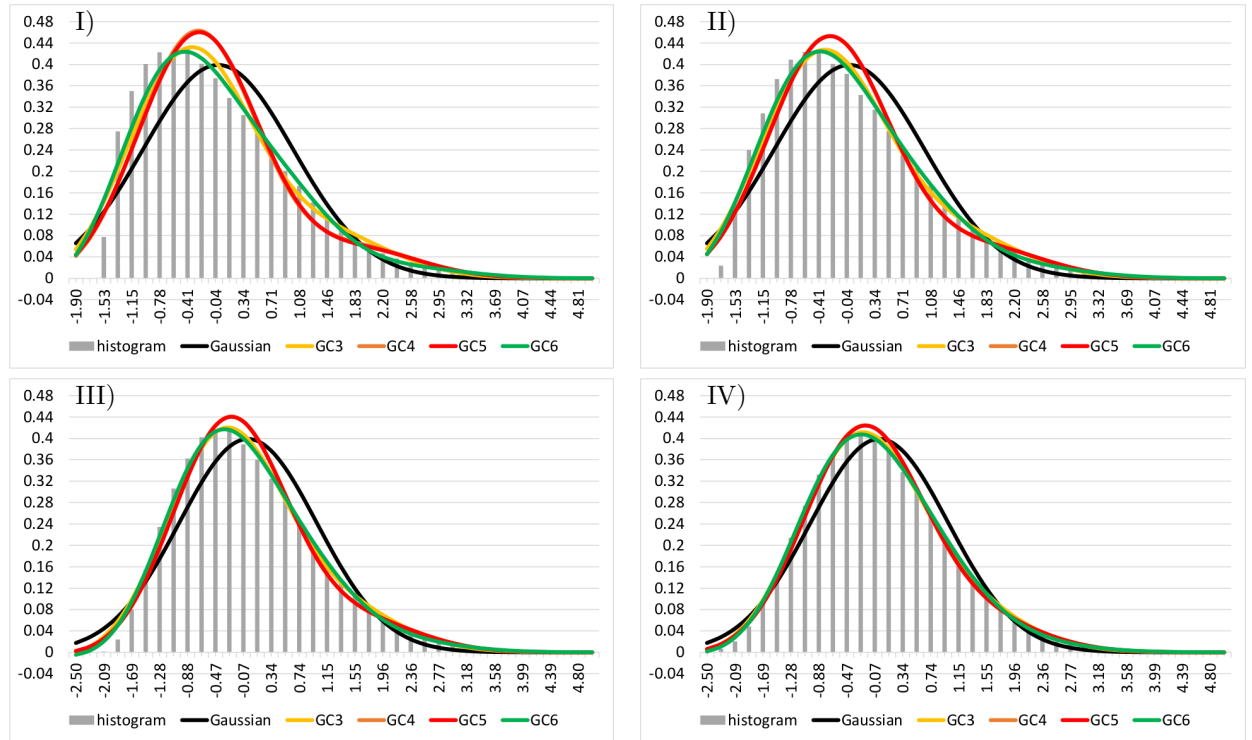


Figure 5: Gram-Charlier expansion of the standardized spatial average for $N = 2$, obtained with SGM. I): $\sigma_\gamma = 1$, II): $\sigma_\gamma = 0.8$, III): $\sigma_\gamma = 0.6$, IV): $\sigma_\gamma = 0.4$.

7.2 Tests with general output distribution

We now investigate how well the GC and ED expansions can approximate a PDF that is not nearly Gaussian. This is achieved with larger values of the input standard deviation than those considered in the previous section. The spatial average 14 and the integral of the square (15) are considered as quantities of interest. With the former, $\sigma_\gamma \in \{0.4, 0.6, 0.8, 1\}$, while with the latter $\sigma_\gamma \in \{1.00, 1.05, 1.10, 1.15\}$. Only the SGM is used, because for the values of σ_γ considered here, the sampling error of the MCM would produce results that are not accurate enough. The value $N = 2$ is chosen for the stochastic dimension. In Table 2 and Table 3, the values of the moments and cumulants are reported for the standardized

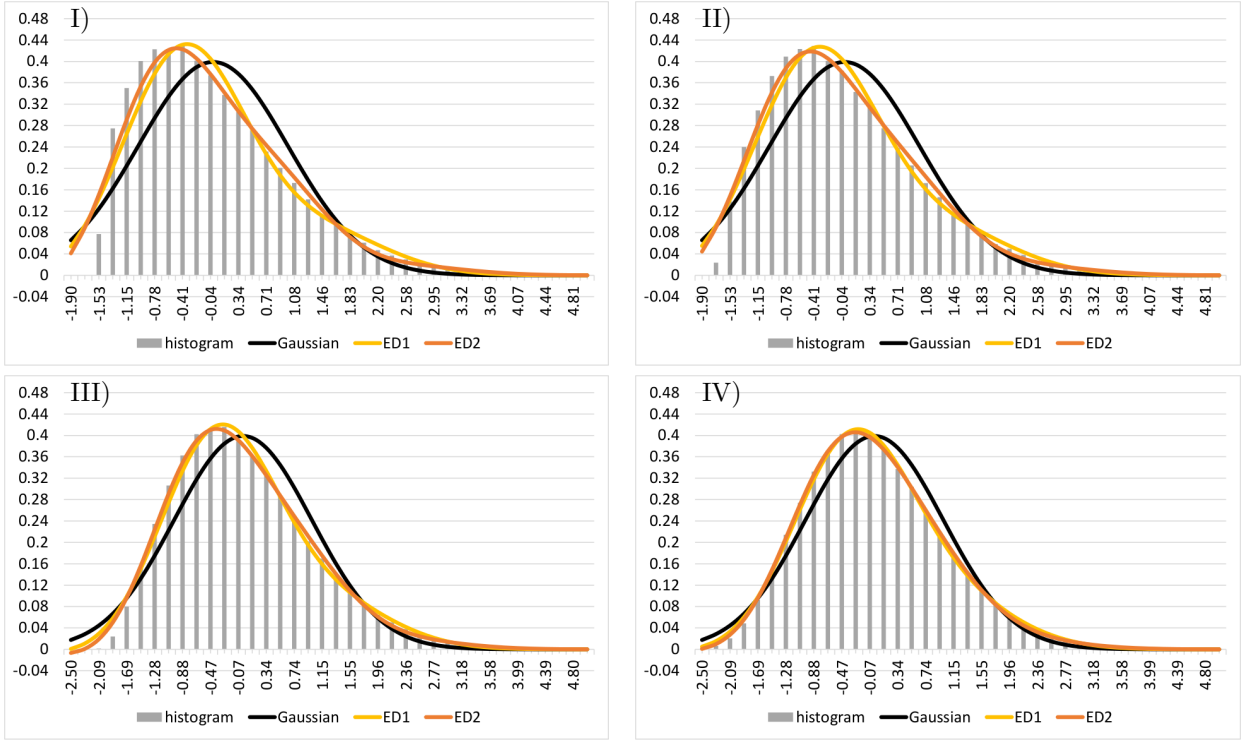


Figure 6: Edgeworth expansion of the standardized spatial average for $N = 2$, obtained with SGM. I): $\sigma_\gamma = 1$, II): $\sigma_\gamma = 0.8$, III): $\sigma_\gamma = 0.6$, IV): $\sigma_\gamma = 0.4$.

spatial average and the standardized integral of the square, respectively. As the input standard deviation grows, all moments increase in magnitude, suggesting that larger values of σ_γ give increasingly non-Gaussian distributions. In Figure 5, the histograms for the spatial average are reported. Larger values of σ_γ produce an increasing positive skewness, and the range of negative values attained by the quantity of interest progressively decreases. The GC curves for the spatial average are in Figure 5. A stronger oscillating behavior with increasing σ_γ can be seen in the pictures. For all values of σ_γ , GC6 provides the best approximation of the PDF, among the GC curves that have been computed. The quality of the approximation slightly decreases as the input standard deviation grows but remains overall satisfactory, especially for lower values of σ_γ . GC3 is also a good approximation, while GC4 and GC5, that lie on top of each other, may be considered good enough only for $\sigma_\gamma = 0.4$. It is possible that, for $\sigma_\gamma = 1$, truncations after GC6 would produce a better approximation, although they have not been computed. In general, since the GC and ED series keep on correcting a standard Gaussian, it could be that more terms are required for a good approximation when the PDF is far from a Gaussian.

The ED results are shown in Figure 6. The best approximation among the curves computed is given by ED2 which well fits all histograms, especially for lower values of the input standard deviation. The quality of the approximation slightly decreases as σ_γ grows, but remains satisfactory. The same behavior was observed for the GC curves. The ED expansions are not qualitatively superior to the GC curves in this case, in the sense that ED2 and GC6 have similar graphs.

Next, we address the case of the integral of the square. The histograms are in Figure 7. Once again, greater values of σ_γ cause an increasing positive skewness, especially going from $\sigma_\gamma = 1.10$ to $\sigma_\gamma = 1.15$. The latter case does not bear any resemblance with a Gaussian distribution, and in fact it is where the computed GC and ED curves struggle more to approximate the behavior of the histogram. The GC curves are in Figure 7. For $\sigma_\gamma = 1.00$, all computed GC curves well approximate the PDF, with GC4 and GC5 lying on top of each other. For $\sigma_\gamma = 1.05$, the best curves are GC4 and GC5, while GC3 and GC6 fail to properly describe the upper part of the histogram. A completely different situation is observed for $\sigma_\gamma = 1.10$, where only GC3 well approximates the histograms, while the other curves fail. It is also worth noticing that GC6 attains negative values: this is expected since the truncated GC and ED expansions are polynomials. Finally, for $\sigma_\gamma = 1.15$, only the GC3 curve is reported, since the other three curves computed showed a divergent behavior. The GC3 curve does a fair job describing the PDF, although it does not reach the maximum value of the histogram. Moreover, it underestimates the PDF in the range $[0.24, 1.52]$ and overestimates it in $(1.52, 365]$.

The ED curves are in Figure 8. ED2 well approximates the histogram for $\sigma_\gamma = 1.00, 1.05$ and 1.10 . For $\sigma_\gamma = 1.15$, ED2 is better than ED1 since it properly describes the top part of the histograms. However,

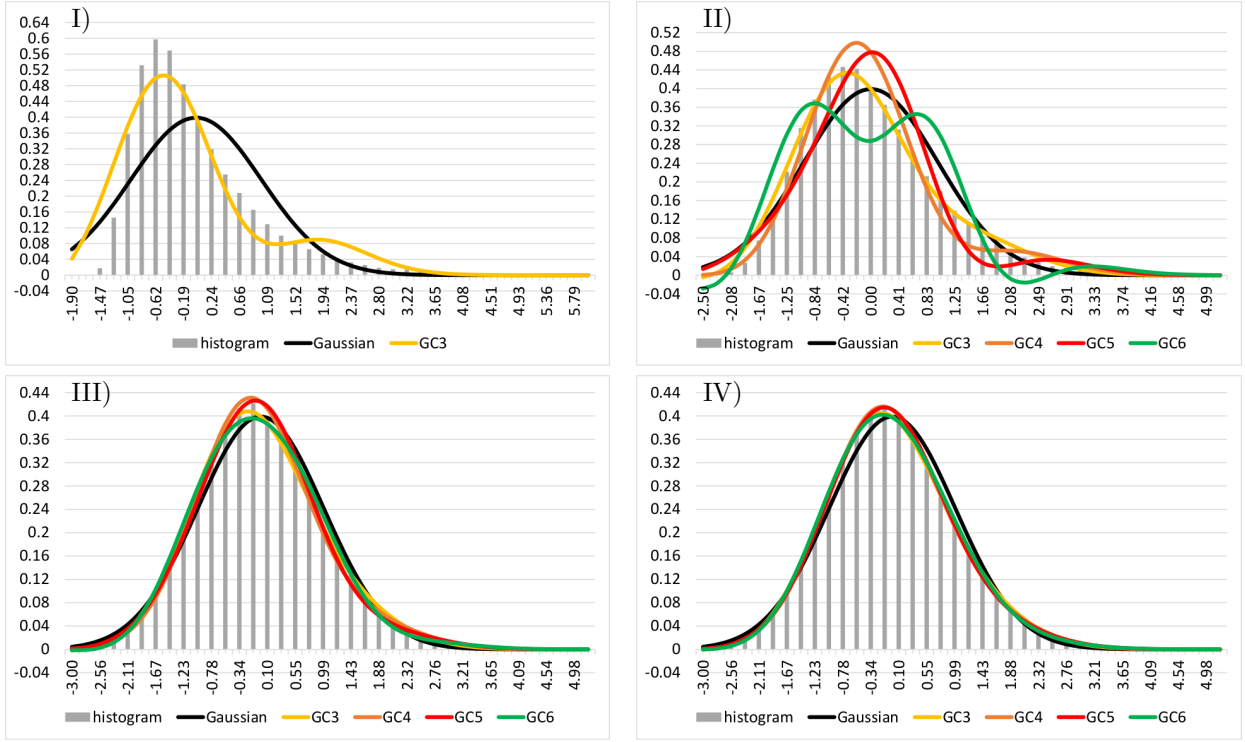


Figure 7: Gram-Charlier expansion of the standardized integral of the square for $N = 2$, obtained with SGM. I): $\sigma_\gamma = 1.15$, II): $\sigma_\gamma = 1.10$, III): $\sigma_\gamma = 1.05$, IV): $\sigma_\gamma = 1.00$.

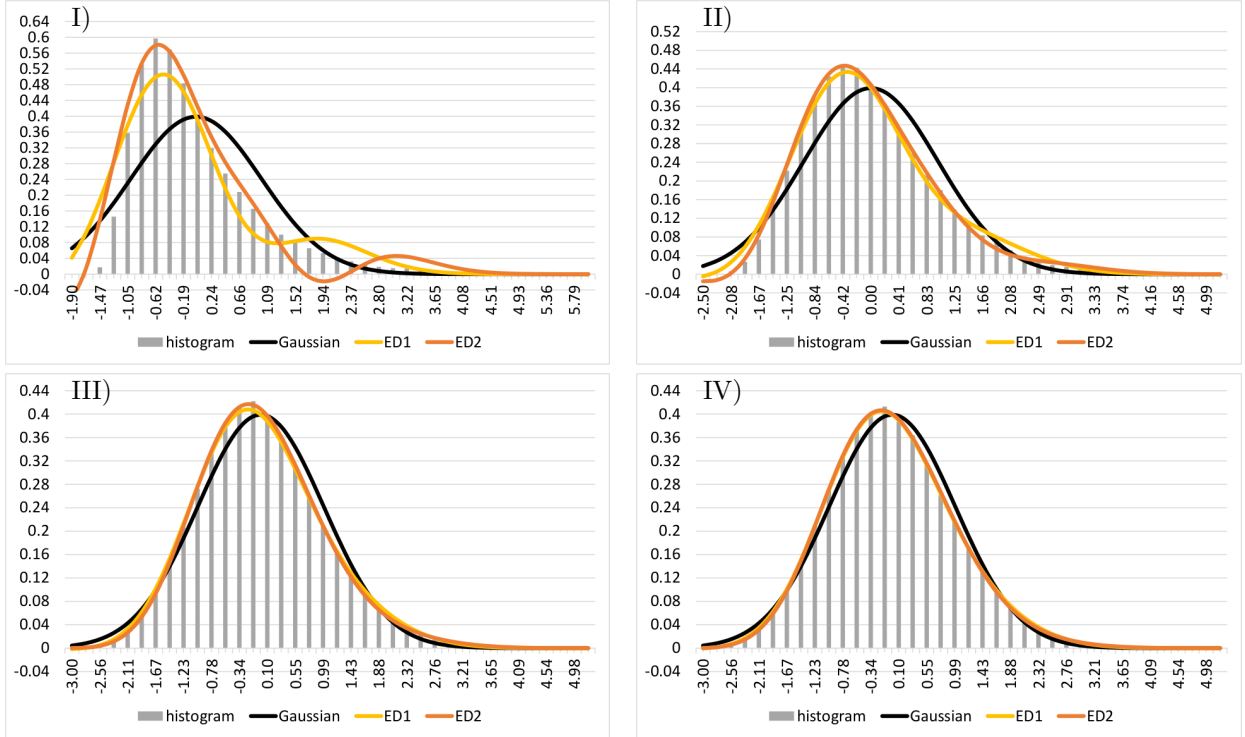


Figure 8: Edgeworth expansion of the standardized integral of the square for $N = 2$, obtained with SGM. I): $\sigma_\gamma = 1.15$, II): $\sigma_\gamma = 1.10$, III): $\sigma_\gamma = 1.05$, IV): $\sigma_\gamma = 1.00$.

also ED2 incurs in an underestimate followed by an overestimate as GC3. Note from Eq. (38) and (45) that GC3 and ED1 are actually the same curve. Because of its broader applicability and accuracy, we conclude that the ED expansion does a much better job than GC for the integral of the square.

8 Discussion

It has been shown that the GC and ED truncated expansions represent a valid alternative to existing methods for the approximation of probability density functions associated with solutions of SPDEs. Our numerical results suggested that GC and ED provide an accurate approximation when the PDF is nearly Gaussian. This is consistent with the nature of the distributions. Even in the case of a general PDF, the truncated expansions well approximated the distributions, especially when the PDF did not deviate too much from a Gaussian. The asymptotic character of the ED expansion makes it more valuable than the GC due to a better monitoring of the error, as the truncation order is increased. Moreover, with PDFs that were far from Gaussian, ED better approximated the distribution than GC, at least up to the truncation order considered in this work.

The proposed method is easy to implement and takes advantage of the fact that exact moments can be computed with the SGM, provided that enough quadrature points are considered. A limitation is the lack of a procedure to determine the necessary number of terms in the truncated series to obtain the best possible approximation. This is inherent in the use of truncated series and the issue is present in all works on ED and GC that we were able to find in the literature. While the optimal number of terms to retain will likely be too large for the desired error in case of a convergent series, it could be theoretically determined a priori in case of an asymptotic expansion such as Edgeworth. Unfortunately, the lack of explicit error bounds make this unfeasible at the moment.

References

- [1] Eugenio Aulisa, Simone Bna, and Giorgio Borna. FEMuS Web page. <https://github.com/eaulisa/MyFEMuS>, 2017.
- [2] Eugenio Aulisa, Giacomo Capodaglio, and Guoyi Ke. Construction of h-refined continuous finite element spaces with arbitrary hanging node configurations and applications to multigrid algorithms. *arXiv preprint arXiv:1804.10632*, 2018.
- [3] Ivo Babuška, Fabio Nobile, and Raul Tempone. A stochastic collocation method for elliptic partial differential equations with random input data. *SIAM Journal on Numerical Analysis*, 45(3):1005–1034, 2007.
- [4] Ivo Babuska, Raul Tempone, and Georgios E Zouraris. Galerkin finite element approximations of stochastic elliptic partial differential equations. *SIAM Journal on Numerical Analysis*, 42(2):800–825, 2004.
- [5] Ivo Babuška, Raul Tempone, and Georgios E Zouraris. Solving elliptic boundary value problems with uncertain coefficients by the finite element method: the stochastic formulation. *Computer methods in applied mechanics and engineering*, 194(12-16):1251–1294, 2005.
- [6] Eric Temple Bell. Partition polynomials. *Annals of Mathematics*, pages 38–46, 1927.
- [7] Mario N Berberan-Santos. Expressing a probability density function in terms of another PDF: A generalized Gram-Charlier expansion. *Journal of Mathematical Chemistry*, 42(3):585–594, 2007.
- [8] Sergei Blinnikov and Richhild Moessner. Expansions for nearly Gaussian distributions. *Astronomy and Astrophysics Supplement Series*, 130(1):193–205, 1998.
- [9] Torgeir Brenn and Stian Normann Anfinssen. A revisit of the Gram-Charlier and Edgeworth series expansions. 2017.
- [10] Susanne Brenner and Ridgway Scott. *The mathematical theory of finite element methods*, volume 15. Springer Science & Business Media, 2007.
- [11] Tan Bui-Thanh, Omar Ghattas, James Martin, and Georg Stadler. A computational framework for infinite-dimensional Bayesian inverse problems part i: The linearized case, with application to global seismic inversion. *SIAM Journal on Scientific Computing*, 35(6):A2494–A2523, 2013.
- [12] Peng Chen and Christoph Schwab. Model order reduction methods in computational uncertainty quantification. *Handbook of Uncertainty Quantification*, pages 1–53, 2016.
- [13] Philippe G Ciarlet. The finite element method for elliptic problems. *Classics in applied mathematics*, 40:1–511, 2002.

- [14] K Andrew Cliffe, Mike B Giles, Robert Scheichl, and Aretha L Teckentrup. Multilevel Monte Carlo methods and applications to elliptic PDEs with random coefficients. *Computing and Visualization in Science*, 14(1):3, 2011.
- [15] Carlo R Contaldi, Rachel Bean, and Joao Magueijo. Photographing the wave function of the universe. *Physics Letters B*, 468(3-4):189–194, 1999.
- [16] Harald Cramér. On the composition of elementary errors: First paper: Mathematical deductions. *Scandinavian Actuarial Journal*, 1928(1):13–74, 1928.
- [17] Harald Cramér. *Mathematical methods of statistics (PMS-9)*, volume 9. Princeton university press, 2016.
- [18] Masoumeh Dashti and Andrew M Stuart. The Bayesian approach to inverse problems. *Handbook of Uncertainty Quantification*, pages 311–428, 2017.
- [19] MB De Kock, HC Eggers, and J Schmiegel. Edgeworth versus Gram-Charlier series: x-cumulant and probability density tests. *Physics of Particles and Nuclei Letters*, 8(9):1023–1027, 2011.
- [20] Valerio B Di Marco and G Giorgio Bombi. Mathematical functions for the representation of chromatographic peaks. *Journal of Chromatography A*, 931(1-2):1–30, 2001.
- [21] Hans C Eggers, Michiel B de Kock, and Jurgen Schmiegel. Determining source cumulants in femtoscopy with Gram-Charlier and Edgeworth series. *Modern Physics Letters A*, 26(24):1771–1782, 2011.
- [22] Miao Fan, Vijay Vittal, Gerald Thomas Heydt, and Raja Ayyanar. Probabilistic power flow studies for transmission systems with photovoltaic generation using cumulants. *IEEE Transactions on Power Systems*, 27(4):2251–2261, 2012.
- [23] George Fishman. *Monte Carlo: concepts, algorithms, and applications*. Springer Science & Business Media, 2013.
- [24] Philipp Frauenfelder, Christoph Schwab, and Radu Alexandru Todor. Finite elements for elliptic problems with stochastic coefficients. *Computer methods in applied mechanics and engineering*, 194(2-5):205–228, 2005.
- [25] Roger G Ghanem and Pol D Spanos. Stochastic finite element method: Response statistics. In *Stochastic Finite Elements: A Spectral Approach*, pages 101–119. Springer, 1991.
- [26] Max D Gunzburger, Clayton G Webster, and Guannan Zhang. Stochastic finite element methods for partial differential equations with random input data. *Acta Numerica*, 23:521–650, 2014.
- [27] Vicente Hernandez, Jose E Roman, and Vicente Vidal. SLEPc: A scalable and flexible toolkit for the solution of eigenvalue problems. *ACM Transactions on Mathematical Software (TOMS)*, 31(3):351–362, 2005.
- [28] SP Huang, ST Quek, and KK Phoon. Convergence study of the truncated Karhunen–Loève expansion for simulation of stochastic processes. *International journal for numerical methods in engineering*, 52(9):1029–1043, 2001.
- [29] Eric Jondeau and Michael Rockinger. Gram-Charlier densities. *Journal of Economic Dynamics and Control*, 25(10):1457–1483, 2001.
- [30] Roman Juszkiewicz, David Weinberg, Piotr Amsterdamski, Michal Chodorowski, and Francois Bouchet. Weakly non-linear Gaussian fluctuations and the Edgeworth expansion. *arXiv preprint astro-ph/9308012*, 1993.
- [31] Maurice G Kendall. *Advanced Theory Of Statistics Vol-I*. Charles Griffin: London, 1943.
- [32] CF Li, YT Feng, DRJ Owen, DF Li, and IM Davis. A Fourier–Karhunen–Loève discretization scheme for stationary random material properties in SFEM. *International journal for numerical methods in engineering*, 73(13):1942–1965, 2008.
- [33] Xiang Ma and Nicholas Zabaras. An efficient Bayesian inference approach to inverse problems based on an adaptive sparse grid collocation method. *Inverse Problems*, 25(3):035013, 2009.

- [34] Youssef M Marzouk, Habib N Najm, and Larry A Rahn. Stochastic spectral methods for efficient Bayesian solution of inverse problems. *Journal of Computational Physics*, 224(2):560–586, 2007.
- [35] Nicholas Metropolis and Stanislaw Ulam. The Monte Carlo method. *Journal of the American statistical association*, 44(247):335–341, 1949.
- [36] Miloud Mihoubi. Bell polynomials and binomial type sequences. *Discrete Mathematics*, 308(12):2450–2459, 2008.
- [37] Trino-Manuel Níguez and Javier Perote. Forecasting heavy-tailed densities with positive Edgeworth and Gram-Charlier expansions. *Oxford Bulletin of Economics and Statistics*, 74(4):600–627, 2012.
- [38] Fabio Nobile, Raul Tempone, and Clayton G Webster. An anisotropic sparse grid stochastic collocation method for partial differential equations with random input data. *SIAM Journal on Numerical Analysis*, 46(5):2411–2442, 2008.
- [39] Fabio Nobile, Raúl Tempone, and Clayton G Webster. A sparse grid stochastic collocation method for partial differential equations with random input data. *SIAM Journal on Numerical Analysis*, 46(5):2309–2345, 2008.
- [40] MCM O’Brien. Using the Gram-Charlier expansion to produce vibronic band shapes in strong coupling. *Journal of Physics: Condensed Matter*, 4(9):2347, 1992.
- [41] Joaquim Olivé and Joan O Grimalt. Gram-Charlier and Edgeworth-Cramér series in the characterization of chromatographic peaks. *Analytica chimica acta*, 249(2):337–348, 1991.
- [42] Jamol Pender. Gram Charlier expansion for time varying multiserver queues with abandonment. *SIAM Journal on Applied Mathematics*, 74(4):1238–1265, 2014.
- [43] Valentin V Petrov. Limit theorems of probability theory: sequences of independent random variables. Technical report, Oxford, New York, 1995.
- [44] Valentin Vladimirovich Petrov. *Sums of independent random variables*, volume 82. Springer Science & Business Media, 2012.
- [45] Ray Popovic and David Goldsman. Easy Gram-Charlier valuations of options. *Journal of Derivatives*, 20(2):79, 2012.
- [46] JM Rickman, A Lawrence, AD Rollett, and MP Harmer. Calculating probability densities associated with grain-size distributions. *Computational Materials Science*, 101:211–215, 2015.
- [47] Mattias Schevenels, Geert Lombaert, and Geert Degrande. Application of the stochastic finite element method for Gaussian and non-Gaussian systems. In *ISMA2004 International Conference on Noise and Vibration Engineering*, pages 3299–3314, 2004.
- [48] Andrew M Stuart. Inverse problems: a Bayesian perspective. *Acta Numerica*, 19:451–559, 2010.
- [49] Daniel M Tartakovsky and Svetlana Broyda. PDF equations for advective–reactive transport in heterogeneous porous media with uncertain properties. *Journal of contaminant hydrology*, 120:129–140, 2011.
- [50] David L Wallace. Asymptotic approximations to distributions. *The Annals of Mathematical Statistics*, 29(3):635–654, 1958.
- [51] Xiaoliang Wan and George Em Karniadakis. An adaptive multi-element generalized polynomial chaos method for stochastic differential equations. *Journal of Computational Physics*, 209(2):617–642, 2005.
- [52] Dongbin Xiu and Jan S Hesthaven. High-order collocation methods for differential equations with random inputs. *SIAM Journal on Scientific Computing*, 27(3):1118–1139, 2005.
- [53] AS Zapevalov, AN Bol’shakov, and VE Smolov. Simulating of the probability density of sea surface elevations using the Gram-Charlier series. *Oceanology*, 51(3):407–414, 2011.